Eur. Phys. J. D **16**, 181–184 (2001)

THE EUROPEAN PHYSICAL JOURNAL D

EDP Sciences

Magnetic excitation of ferromagnetic dimer molecules

T. Oda[a]

Department of Computational Science, Faculty of Science, Kanazawa University, Kanazawa 920-1192, Japan

Received 29 November 2000

Abstract. The magnetic excitation in ferromagnetic dimer molecules was studied with using the local spin-density approximation. The equation of motion for the atomic magnetic moment was presented. To obtain adiabatic excited states, we implemented a penalty energy technique, which imposes a frozen spin configuration. Calculation conditions of the technique were examined. We applied the method to ferromagnetic dimer molecules, Fe_2, and estimated the magnetic excitation energy. We discussed the magnetic interaction between atoms with mapping the result onto the Heisenberg model.

PACS. 31.50.+w Excited states – 31.15.Ar Ab initio calculations – 71.15.Pd Molecular dynamics calculations (Car-Parrinello) and other numerical simulations – 75.50.Bb Fe and its alloys

1 Introduction

Magnetic properties have been often studied by using the Heisenberg model, which is useful on various magnetic materials. The mapping of system to a Heisenberg model would be an interesting subject on the magnetic materials also in many *ab initio* approaches [1,2]. Once the mapping has been done, magnetic properties are derived from the model Hamiltonian. Alternatively, there would be a way to treat the system only from first principles. Recently, the magnetic corrective excitation energy are discussed with the time-dependent variational principle by Niu and Kleinman [3]. Following their work, the magnetic excitation which causes the adiabatic slow dynamics can be described by a new equation, which we call the Niu-Kleinman (NK) equation in this paper. The application to the Kohn-Sham (KS) density functional theory [4] is straightforward and, without mapping to a Heisenberg model, gives the quantitative discussion on the low-lying magnetic excitation of system in the *ab initio* manner.

In this paper, we described the theory for estimating the magnetic excitation energy of ferromagnetic dimer in the density functional theory and applied it to the molecule, Fe_2. The checking of calculations and the comparison with the result obtained from the Heisenberg model have been performed. The magnetic cluster, Fe_2, has a ferromagnetic ground state with the total magnetization and the bond length being $6\mu_B$ and 3.70 a.u., respectively. These properties are experimentally observed [5,6]. Based on adiabatic treatments for the magnetic excitation, frozen magnon calculations have been performed with the local spin-density approximation (LSDA) or its gradient corrected one for the bulk of magnetic elements (Fe, Co, Ni) [7,8] and the antiferromagnet MnO [9].

[a] e-mail: oda@cphys.s.kanazawa-u.ac.jp

2 Theory

2.1 Niu-Kleinman equation for ferromagnetic dimers

The NK equation describes dynamics of slow variables for the magnetic excitation. Slow variables of electronic freedom can be separated from the high energy excitation by imposing an adiabatic approximation. Suppose that the ground state Φ_0 of system realizes the ferromagnetic spin configuration of a dimer molecule. For example, the Φ_0 is a single Slater determinant consisting of a set of occupied Kohn-Sham orbitals with bispinor representation. The magnetization density $\mathbf{m}(\mathbf{r})$ is calculated from $\langle\Phi|\rho(\mathbf{r})\boldsymbol{\sigma}|\Phi\rangle$, where $\rho(\mathbf{r})$ and $\boldsymbol{\sigma}$ is the density operator and the Pauli's spin vector. The magnetization density of the ground state, $\mathbf{m}_0(\mathbf{r})$, is obtained from this expression with the wave function $\Phi = \Phi_0$. Low-energy magnetic excitations are identified with the small deviation from the ground state magnetization density.

The wavefunction of the excited state, within the adiabatic approximation, was defined as the wavefunction which minimizes the total energy of system subject to the constraint imposed on a magnetization configuration (frozen spin approximation). Then, these wavefunctions are functionals of magnetization densities, namely, $\Phi = \Phi[\mathbf{m}(\mathbf{r})]$.

Equations of motion for the magnetization would be obtained by employing the time-dependent variational principle [10] that the action should be extremized by the wavefunction with the frozen spin approximation. With adding the harmonic approximation in the magnetization deviation, the equation of motion for the magnetization should be obtained in general [3,8].

The magnetization density is distributed around atoms with a shape at the ground state and rigidly canted at low-energy excited states deviated from the ground state.

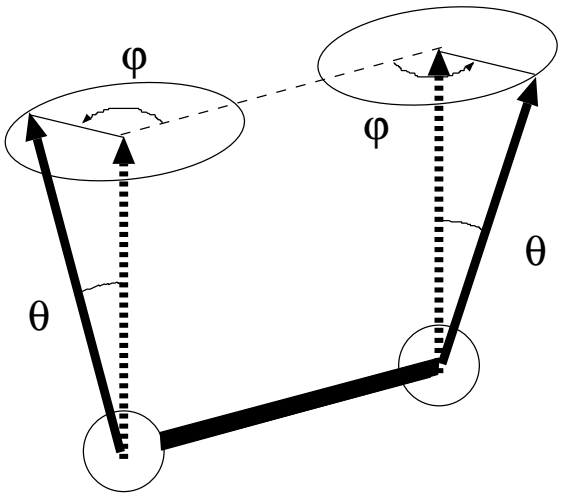

Fig. 1. The spin configuration of the adiabatic magnetic excitation.

In many cases of the magnetic real system, the atomic magnetic moment may be a well defined quantity when an appropriate atomic region is specified. Introduce the atomic magnetic moment given by

$$\mathbf{M}_{\mathrm{I}} = \mu_{\mathrm{B}} \int_{V_{\mathrm{I}}} \mathbf{m}(\mathbf{r}) d\mathbf{r}, \tag{1}$$

where the atomic region of Ith atom, V_{I}, was defined by the sphere with a radius, $r_{\mathrm{a}}^{\mathrm{I}}$, and the μ_{B} is the Bohr magneton. Choosing the z-axis as a quantized axis, $\mathbf{M}_{\mathrm{I}} = M\mathbf{e}_z$ for both atoms in the ground state of molecule. The low-lying magnetic excitations are described by two cooperative magnetic modes,

$$M_x = M_{1x} - M_{2x}, \tag{2}$$
$$M_y = M_{1y} - M_{2y}. \tag{3}$$

Within the harmonic approximation, the modulus of magnetization does not change from the ground state value. It may be convenient to use polar coordinates (see Fig. 1) for the modes

$$\frac{1}{2M}\begin{pmatrix} M_x \\ M_y \end{pmatrix} = \theta \begin{pmatrix} e_m^x \\ e_m^y \end{pmatrix} = \theta(\cos\phi\ \mathbf{e}_x + \sin\phi\ \mathbf{e}_y), \tag{4}$$

where $\mathbf{e}_x$ and $\mathbf{e}_y$ are unit vectors along x- and y-direction of spin space. The θ and ϕ represent the polar angle of the adiabatic magnetic moment from the z-axis and the rotated angle from the x-axis. The time-derivative of the latter gives the angular frequency of the magnetic excitation. The θ, which is assumed to be a small value, will be used for the intermediate parameter in the frozen spin calculation.

The NK equation is given by

$$\hbar \begin{pmatrix} \Omega_{xx}\ \Omega_{xy} \\ \Omega_{yx}\ \Omega_{yy} \end{pmatrix} \begin{pmatrix} \dot{e}_m^x \\ \dot{e}_m^y \end{pmatrix} = \begin{pmatrix} K_{xx}\ K_{xy} \\ K_{yx}\ K_{yy} \end{pmatrix} \begin{pmatrix} e_m^x \\ e_m^y \end{pmatrix}, \tag{5}$$

where

$$\Omega_{\alpha\beta} = -2\mathrm{Im}\left\langle \frac{\partial \Phi}{\partial \mathbf{e}_\alpha} \middle| \frac{\partial \Phi}{\partial \mathbf{e}_\beta} \right\rangle \tag{6}$$

and

$$K_{\alpha\beta} = \frac{\partial^2 E_{tot}}{\partial \mathbf{e}_\alpha \partial \mathbf{e}_\beta} \tag{7}$$

for $\alpha, \beta = x, y$. The diagonal part of $\Omega_{\alpha\beta}$ vanishes and the off-diagonal part has an anti-symmetry, $\Omega_{xy} = -\Omega_{yx}$. Since the spin-orbit interaction is neglected at present case, the spin configuration is equivalent under rotations around the z-axis. Therefore, $K_{xx} = K_{yy}$ and $K_{xy} = K_{yx} = 0$. For the eigen spin configurations, $e_m^{\pm} = e_m^x \pm i e_m^y$, the eigenenergy is given by

$$\hbar\omega = \pm \frac{K_{xx}}{\Omega_{xy}}, \tag{8}$$

where the $\pm$ corresponds to the signs of precession of the atomic magnetic moment. In the frame of frozen spin calculations, the minimum total energy and the corresponding wave functions are required to calculate under the constraint with a finite θ. When we write them as $E[\theta\mathbf{e}_\alpha]$ and $\Phi[\theta\mathbf{e}_\alpha]$, the excitation energy is estimated from

$$|\hbar\omega| = \frac{E[\theta\mathbf{e}_x] - E[0]}{|\Delta\Omega[\theta\mathbf{e}_x, \theta\mathbf{e}_y]|}, \tag{9}$$

where

$$\Delta\Omega[\theta\mathbf{e}_x, \theta\mathbf{e}_y] = -2\mathrm{Im}\langle\, \Phi[\theta\mathbf{e}_x] - \Phi[0] \,\big|\, \Phi[\theta\mathbf{e}_y] - \Phi[0] \,\rangle. \tag{10}$$

We should note three points here. First, both denominator and numerator of Eq. (9) are proportional to the square of θ for small θs. Therefore, the $\hbar\omega$ calculated dose not strongly depend on the θ used. Next, the definition of $\Delta\Omega$ contains the difference of wavefunction. Due to this, even the phase of $\Phi[\theta\mathbf{e}_\alpha]$ should continuously tend to the phase of $\Phi[0]$ when θ goes to zero. Finally, both of $\Phi[\theta\mathbf{e}_x]$ and $\Phi[\theta\mathbf{e}_y]$ are not necessarily obtained from the energy minimization under respective constraints. One connects with the other by a rotation of the spin space.

Alternatively, $\Delta\Omega$ can be expressed by using a Berry phase representation [11],

$$\Delta\Omega[\theta\mathbf{e}_x, \theta\mathbf{e}_y] = -2\ \mathrm{Im}\log\langle\, \Phi[0] \,\big|\, \Phi[\theta\mathbf{e}_x] \,\rangle \times \langle\, \Phi[\theta\mathbf{e}_x] \,\big|\, \Phi[\theta\mathbf{e}_y] \,\rangle \langle\, \Phi[\theta\mathbf{e}_y] \,\big|\, \Phi[0] \,\rangle. \tag{11}$$

This expression may be convenient for numerical estimation. Because each wave function and its complex conjugate appear in the expression, it is not necessary to take care of arbitrary phases of wave functions.

2.2 Spin constraint

The adiabatic wave function and the adiabatic potential energy were estimated by the spin constraint technique

with a penalty energy function. Introduce the penalty energy,

$$E_{\rm p} = \frac{1}{2}\int \alpha(\mathbf{r})(\mathbf{m}^{\perp}(\mathbf{r}))^2 d\mathbf{r}, \tag{12}$$

where $\mathbf{m}^{\perp}$ represents the spin density component perpendicular to the constraint direction $\mathbf{e}_{\rm c}(\mathbf{r})$ and the $\alpha(\mathbf{r})$ is a sufficiently large positive value. The energy minimization of the total energy which includes the penalty energy allows us to impose a constraint on the spin configuration. Further, taking into account a distribution of the spin density around atoms, we introduce the approximation,

$$\alpha(\mathbf{r}) = \begin{cases} \alpha_{\rm I} & |\mathbf{r}-\mathbf{R}_I| < r_a^I \\ 0 & \text{otherwise,} \end{cases} \tag{13}$$

where the penalty parameter α_I is uniformly constant around the atomic site $\mathbf{R}_I$. The penalty energy is finally expressed by

$$E_{\rm p} = \frac{1}{2}\sum_I \alpha_I \int_{V_{\rm I}} (\mathbf{m}_I^{\perp}(\mathbf{r}))^2 d\mathbf{r}. \tag{14}$$

To get the adiabatic state, after obtaining the ground state spinor wave functions, we switched gradually on the constraint. In practice, we used the formula of molecular dynamics,

$$\mu\ddot{\Psi}_i(\mathbf{r}) = -\mathcal{H}\Psi_i(\mathbf{r}) - \frac{\delta E_{\rm p}}{\delta\Psi_i(\mathbf{r})} + (\text{damping}) + (\text{orthogonalization constraint}), \tag{15}$$

in the update of wave functions, where Ψ and $\mathcal{H}$ is the KS wave function and the KS Hamiltonian with spinor representation and μ is the pseudo mass for the freedom of wavefunctions [12–14]. We start with very small θ and α_I, and, during appropriate times of updates, increase these values to interested values. For the θ, we mainly used 3° and tested 2° and 5°. The larger constraint parameter α_I would be expected to give more accurate results.

3 Application to Fe_2

3.1 Result

The Fe_2 molecule, whose bond length was fixed at the ground state value, was set in a large periodic cubic box having the dimension of 20 a.u. The ultra-soft pseudopotentials were employed to describe the valence-core interaction [14–16]. In this pseudo-potential scheme the density matrix has a hard augmented component, for which we used a cutoff energy of more than 250 Ry. The spinor wave functions were expanded by a cutoff energy of more than 24 Ry. The convergence with respect to these cutoff energies was examined. The formula given by Perdew and Zunger [17] was used for the exchange-correlation energy.

The excitation energy was directly estimated by Eq. (9), in which the numerator was obtained from the difference of total energies between the ground state and the adiabatic state, ΔE, and the denominator, $\Delta\Omega$, was calculated by using the KS wave functions. ΔE and $\Delta\Omega$ were expected to be proportional to the square of θ. Figure 2 shows ΔE and $\Delta\Omega$ with respect to θ^2. The excitation energies are 558, 555 and 556 meV for $\theta = 2°, 3°$, and 5°, where $\alpha_{\rm I} = 6400$ a.u. and $r_{\rm a} = 1.5$ a.u. were used.

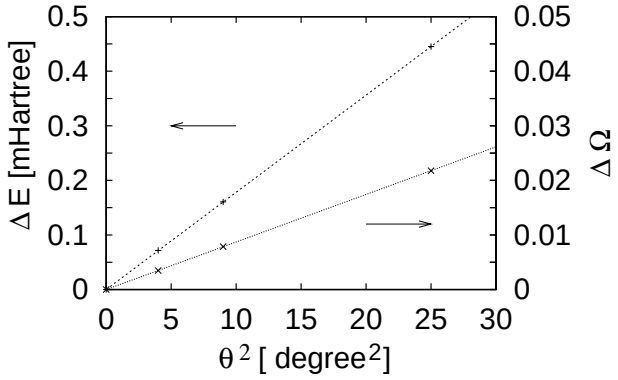

Fig. 2. The typical θ-dependence of the ΔE and $\Delta\Omega$. $\alpha_{\rm I} = 6400$ a.u. and $r_{\rm a} = 1.5$ a.u. were used.

The resulting penalty energies (= $E_{\rm p}$) were within several percent of ΔE. Consequently, the excitation energy was obtained within several percent for $\alpha_{\rm I}$ parameters (800 $\sim$ 6400 a.u.) used in the present work. We tested the dependence of the radius of atomic spheres, $r_{\rm a}$. When the radius is between 75 and 85% of the half of bond length, the resulting excitation energy falls within several percents of the value at $r_{\rm a} = 1.5$ a.u. The modulus of atomic moments calculated dose not change from the ground state value even for $\theta = 5°$.

The other important parameter of calculation conditions is a cutoff of the plane waves. The test of cutoff energies are shown in Fig. 3. The full and dotted curves represent convergences with respect to $E_{\rm cut}^{\rm WF}$ and $E_{\rm cut}^{\rm dens}$, respectively. As written in the figure, the Ω_{xy} (= $\Delta\Omega/\theta^2$) shows a good convergence with respect to $E_{\rm cut}^{\rm WF}$ and $E_{\rm cut}^{\rm dens}$. Changes of $\hbar\omega$ in the figure are mainly caused by K_{xx}. The convergence of K_{xx} with respect to $E_{\rm cut}^{\rm WF}$ is relatively slow. When $E_{\rm cut}^{\rm WF} = 60$ Ry, the $E_{\rm p} = 0.0025$ mHartree, which is 1.7% of ΔE.

3.2 Discussion

It is interesting to map the results onto a Heisenberg model,

$$H = J\mathbf{S}_1 \cdot \mathbf{S}_2, \tag{16}$$

where J is the exchange-interaction between two atomic moments. The magnetic excitation energy is given by $\hbar\omega = \pm 2\mu_{\rm B}|J|S$, where S is the atomic moment of the model, while the variation of magnetic energy with respect to the frozen spin configuration is given by $\Delta E(\theta) = 2|J|S^2\theta^2$. The resulting expression for $\hbar\omega$ is

$$|\hbar\omega| = \frac{\mu_{\rm B}}{S}\frac{\Delta E(\theta)}{\theta^2}. \tag{17}$$

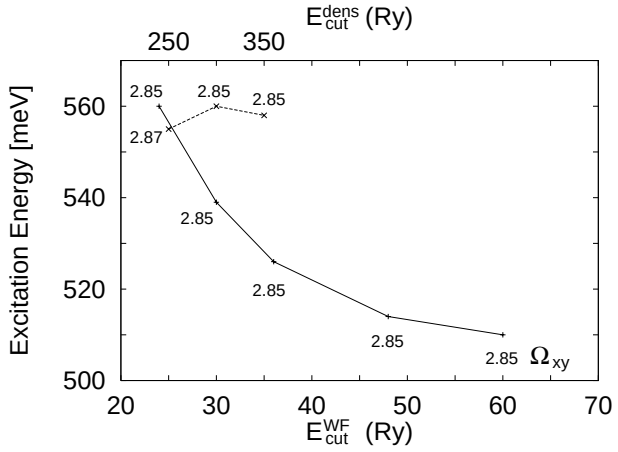

Fig. 3. The convergence of the excitation energy with respect to $E_{\rm cut}^{\rm WF}$ (full curve, $E_{\rm cut}^{\rm dens} = 300$ Ry) and $E_{\rm cut}^{\rm dens}$ (dotted curve, $E_{\rm cut}^{\rm FW} = 24$ Ry). The data of Ω_{xy} are written in the figure. $\theta = 3^\circ$, $\alpha_I = 6400$ a.u., and $r_{\rm a} = 1.5$ a.u. were used.

The comparison with Eq. (9) implies that $|\Delta\Omega|/\theta^2 \sim S/\mu_{\rm B}$. Indeed, Ω_{xy} $(= |\Delta\Omega|/\theta^2)$ is estimated to be 2.85, which is close to the value of total magnetic moment per atom in $\mu_{\rm B}$.

Suppose spin rotation operators, $U_\alpha(\theta)\,(\alpha = x, y)$, about α-axis by the angle, θ, at each point in real space. After introducing KS orbitals $\{\Psi_i\}$ in Eq. (10) or (11) and using the spin rotation operator to construct adiabatic wave functions, $\Phi[\theta \mathbf{e}_\alpha]$, it is found that $|\Delta\Omega| \simeq M_{\rm tot}\theta^2/2\mu_{\rm B}$, where $M_{\rm tot}$ is the total magnetic moment. This relation may give a qualitative validity for using a Heisenberg model in the system. However, quantitatively, there are ambiguities in using $M_{\rm total}/2\mu_{\rm B}$ or $M/\mu_{\rm B}$ instead of Ω_{xy}. Our result shows that Ω_{xy} dose not strongly depend on the calculation conditions. For example, Ω_{xy} under $r_{\rm a} = 1.0$ a.u. is smaller than the value of $r_{\rm a} = 1.5$ a.u. by only 4%, whereas the calculated atomic moment, M, under $r_{\rm a} = 1.0$ a.u. is even smaller than the value at $r_{\rm a} = 1.5$ a.u. by 28%.

Within the Heisenberg model, the difference between energies of the ferro- and antiferromagnetic configurations allows us to make an estimation of the exchange interaction between atomic moments. The antiferromagnet has an energy above the ferromagnet by 1.91 eV, which is in agreement with the previous value, 2.10 eV [18]. Consequently, $|J|S^2 \simeq \frac{1}{2} \times 1.91$ eV $= 955$ meV. This value is larger than $|J|M^2 (= \Delta E(\theta)/2\theta^2 = 727$ meV) calculated in the frozen spin calculation by about 30%. We should note that the latter presents the interaction related only with the ground state, but the former includes some averaged effects between the ferro- and antiferromagnetic states.

The converged value of magnetic excitation energy is expected from the limit of the large $E_{\rm cut}^{\rm WF}$ in Fig. 3 to be 508 meV. This value is similar to the maximum magnon energy calculated by Halilov *et al.* in the bulk bcc Fe [7].

4 Summary

We have implemented the *ab initio* approach to the magnetic excitation energy, based on the time-dependent variational principle and the adiabatic approximation for electronic slow variables. The application to Fe_2 molecule was performed with help of the constraining technique that we have developed. The calculation condition of the method developed in this work was examined. The convergence of the magnetic excitation energy with respect to the cutoff energy is slow and $E_{\rm cut}^{\rm WF} = 60$ Ry is necessary to the accuracy of a few percent. The calculated Berry curvature, Ω_{xy}, dose not strongly depend on the calculation conditions. Therefore, the ambiguity by mapping to the Heisenberg model, which may be around 30% in the magnetic excitation energy, will be almost avoided by using the Berry curvature. The observation of the magnetic excitation studied in this work is desired in experiments.

The author would like to thank Profs. R. Car and N. Suzuki and Drs. A. Pasquarello and H. Nagao for discussions. The present work was supported by a Grant-in-Aid for Scientific Research provided by the Ministry of Education, Science, Sports and Culture, Japan.

References

1. T. Oguchi, K. Terakura, N. Hamada, J. Phys. F: Met. Phys. **13**, 145 (1983).
2. A.I. Liechtenstein, M.I. Katsnelson, V.P. Antropov, V.A. Gubanov, J. Magn. Magn. Mat. **67**, 65 (1987).
3. Q. Niu, L. Kleinman, Phys. Rev. Lett. **80**, 2205 (1998).
4. P. Hohenberg, W. Kohn, Phys. Rev. B **136**, 864 (1964); W. Kohn, L.J. Sham, Phys. Rev. A **140**, 1133 (1965).
5. H. Purdum, P.A. Montano, G.K. Shenoy, T. Morrison, Phys. Rev. B **25**, 4412 (1982).
6. D.M. Cox, D.J. Trevor, R.L. Whetten, E.A. Rohlfing, A. Kaldor, Phys. Rev. B **32**, 7290 (1985).
7. S.V. Halilov, H. Eschrig, A.Y. Perlov, P.M. Oppeneer, Phys. Rev. B **58**, 293 (1998).
8. R. Gebauer, S. Baroni, Phys. Rev. B **61**, R6459 (2000).
9. I.V. Solovyev, K. Terakura, Phys. Rev. B **58**, 15496 (1998).
10. K.L. Liu, S.H. Vosko, Can. J. Phys. **67**, 1015 (1989).
11. R. Resta, Rev. Mod. Phys. **66**, 899 (1994).
12. R. Car, M. Parrinello, Phys. Rev. Lett. **55**, 2471 (1985).
13. F. Tassone, F. Mauri, R. Car, Phys. Rev. B **50**, 1056 (1994).
14. T. Oda, A. Pasquarello, R. Car, Phys. Rev. Lett. **80**, 3622 (1998).
15. D. Vanderbilt, Phys. Rev. B **41**, 7892 (1990).
16. K. Laasonen, A. Pasquarello, R. Car, C. Lee, D. Vanderbilt, Phys. Rev. B **47**, 10142 (1993).
17. J.P. Perdew, A. Zunger, Phys. Rev. B **23**, 5048 (1981).
18. J.L. Chen, C.S. Wang, K.A. Jackson, M.R. Pederson, Phys. Rev. B **44**, 6558 (1991).